The Extraction of Urban Built-Up Areas by Integrating Night-Time Light and POI Data—A Case Study of Kunming, China

ZHANG JUN[ID], YUAN XIAO-DIE, AND LIN HAN
School of Architecture and Planning, Yunnan University, Kunming 650500, China
Corresponding author: Zhang Jun (luzhang121@163.com)

ABSTRACT With the urban built-up area becoming one of the most prominent forms of urban expansion, accurately extracting the urban built-up area is becoming more and more important to judge the urbanization process and evaluate the urban environment. Since it is difficult to significantly improve the accuracy of single satellite data in the extraction of urban built-up areas, this study proposes a method integrating POI (Point of Interest) data and Luojia-1A data to improve the extraction accuracy of urban built-up areas. In this study, integrated Density Graph, OSTU and geometric mean are used to extract urban built-up areas respectively. The highest precision of urban built-up areas extracted before data integration is 74.3% with the highest Kappa value of 0.54; while the highest precision of urban built-up area extracted after data integration is 91.4%, with the highest Kappa value of 0.91. Therefore, it can be concluded that compared with the existing widely used night-light-based methods, this method can integrate the advantages of POI data and Luojia-1A data, that is, it can not only solve the long-term oversaturation phenomenon of night light data, but also can extract urban built-up areas in a more refined way. The method used in this study, which integrates POI data and Luojia-1A data, can not only provide a new method for urban built-up area extraction, but also can play an active guiding role in urban planning and construction.

INDEX TERMS Urban expansion, LuoJia-1A, data integration, urban space, urban morphology.

I. INTRODUCTION

In recent decades, with the rapid urbanization of China and the intensification of agricultural modernization in urban built-up areas, cities have undergone unlimited expansion, and changes have also occurred [1], [2]. Urban built-up areas are the carrier of all urban activities, the main gathering areas for the population and economic activities, and a prominent manifestation of urbanization [3], [4]. The implementation of "national spatial planning" in China clearly proposes the demarcation of the boundary line between urban and rural areas [5], [6]. Therefore, the extraction of urban built-up areas has become increasingly important.

The urban built-up area refers to the expropriated land and the non-agricultural production construction area developed by actual construction within the municipal administrative area, which includes the concentrated part of the urban area and the urban construction land that is scattered in the suburban area but has close contact with the city

The associate editor coordinating the review of this manuscript and approving it for publication was Wenming Cao[ID].

and has basically improved and perfected municipal public facilities [7]. At present, the extraction and division of urban built-up areas in China mainly depends on the guidance of the government's statistical yearbook and planning documents, but these resources cannot truly and objectively reflect the scope of urban built-up areas [8]. This study aims to further improve the extraction effect of urban built-up areas through data integration based on existing research.

II. LITERATURE REVIEW

A. RESEARCH ON NIGHT-TIME LIGHT DATA

Night-time light remote sensing data, which reflect the function of urban infrastructure through the brightness of urban night-time lights, are basic data that are widely used in relevant urban research [9], [10]. To some extent, night-time light data can compensate for the lack of panel statistical data in urban space research. Moreover, night-time light data can be applied in the study of urban space [11] because urban activities are closely correlated with electricity consumption [12], and many studies have proven that the intensity of urban light

has a high correlation with urban population distribution [13]. Therefore, night-time light data are currently mainly used in urban expansion [14], urban morphology and structure [15], and social and economic status decisions [16].

In research on urban spatial structure, researchers have tested the relationship between urban residential areas and rural areas [17] by using DMSP/OLS ((Defense Meteorological Satellite Programmed/Operational Lines can System)) data. Yu developed a new object-oriented method in 2014 to characterize the urban model for the analysis of night satellite images [18], moreover, VIIRS (visible infrared imaging radiometer) data make it possible to examine the urban internal spatial structure in more detail [19], Furthermore, subsequent scholars have also conducted studies on urban spatial structure with finer resolution [20] based on VIIRS data, including the re-evaluation of social and economic indicators [21] and detection of urban internal regional structure [22].

The LuoJia-1A night-time light image, newly released by Wuhan University in 2018, has a spatial resolution of 130 meters and can more clearly reflect the night-time structure of a city [23]. Although night-time light data have a relatively higher spatial stability than other types of data and retain the integrity of the study area as much as possible, night-time light sensors cannot record socio-economic attributes and human daily activities [11], [24], [25]. Moreover, the sensors record not only strong light emitted by a city but also strong light emitted by airports, roads, ports, etc., which further leads to the inaccurate judgement of urban areas [26], [27].

B. APPLICATION OF POI DATA

amount of big data has begun to be applied to the study of cities [28], including network review data [29], social software data [30], Internet data [31], thermal graph data [32], POI data [33], dating data [34], IC card data [35], mobile phone signal data [36] and GPS data [37] and so on. The influences of these factors on the spatial connection of cities [38], the functional layout of cities [39], and the behavioral space of cities [40] have been studied in detail. These studies show that big data have higher adaptability in urban space research than traditional data [41], [42].

POI (point of interest) data express all urban entity abstractions in virtual geographic space and have the advantages of high accuracy, fast data update speed and large data volume etc., so big data have been widely used as new geospatial data in recent years [43], [44]. At present, POI data are mainly used to determine the spatial structure of cities, including the extraction of urban centres [45], the distribution of urban facilities [46], the division of urban functions [47], and the analysis of spatial patterns [48]. Compared with traditional data, POI data research in urban space has the advantages of higher speed and better accuracy [49]; however, there are relatively few studies on the application of POI data in the extraction of urban built-up areas. Some scholars have extracted the abrupt character of POI data at the city boundary [50] and summarized the general threshold value of POI data to deduce the city boundary in Chinese cities. POI data are

also used to extract the main built-up areas of cities with high agglomeration in urbanization [50]. However, due to the high-density difference between the number of POIs in built-up and non-built-up urban areas, it is easy to make errors [47].

C. RESEARCH ON DATA INTEGRATION

Although an increasing number of scholars have begun to pay close attention to the application of data integration in urban cities and there have also been studies showing that night-time light data and POI data have a strong coupling relationship in urban spaces [51], there are still few studies on the integration of night-time light data and POI data, let alone the use of data integration to extract urban built-up areas [52]. To extract the urban built-up areas of Kunming, China, which have undergone drastic changes, this study attempts to integrate POI data with night-time light data.

It is also hoped that a new method can be used to integrate POI data and night light data to explore the improvement of the accuracy of urban built-up area extraction by data integration on the basis of comparing the results of different data extraction of urban built-up area.

III. RESEARCH AREA AND RESEARCH DATA
A. RESEARCH AREA

Kunming, the provincial capital of Yunnan Province, is one of the most urbanized cities in western China. With the development and promotion of national macro strategies such as "One Belt and One Road" and "western development", the urban built-up area of Kunming has expanded significantly in recent years [53]. According to the statistical yearbook of Yunnan Province in 2019, the urbanization rate of Kunming's main urban area exceeded 70% in 2019. As the provincial capital city, Kunming has a relatively perfect urban economic structure, social structure and spatial structure with complete urban functions and configurations in terms of economy, culture, transportation and other aspects. The research area of this study is the main urban area of Kunming (including 5 administrative districts, FIGURE 2. **POI Data (a) and LuoJia-1A Data (b) of 2019**). The reason why the research area does not include other districts and counties except the main urban area is mainly due to the significantly lower area of urban built-up areas of other districts and counties compared with the main urban area.

B. RESEARCH DATA
1) LUOJIA-1A DATA

The night-time light data used in this study are derived from the LuoJia-1A scientific experiment satellite launched by Wuhan University of China, with a spatial resolution of 130 meters. The main reasons for choosing LuoJia-1A night-time. light data in this study are as follows. First, the use of LuoJia-1A night-time light data greatly improves the time and spatial resolution of night-time light data. Second, the use of these data improves some problems with traditional night-time light data, including the low
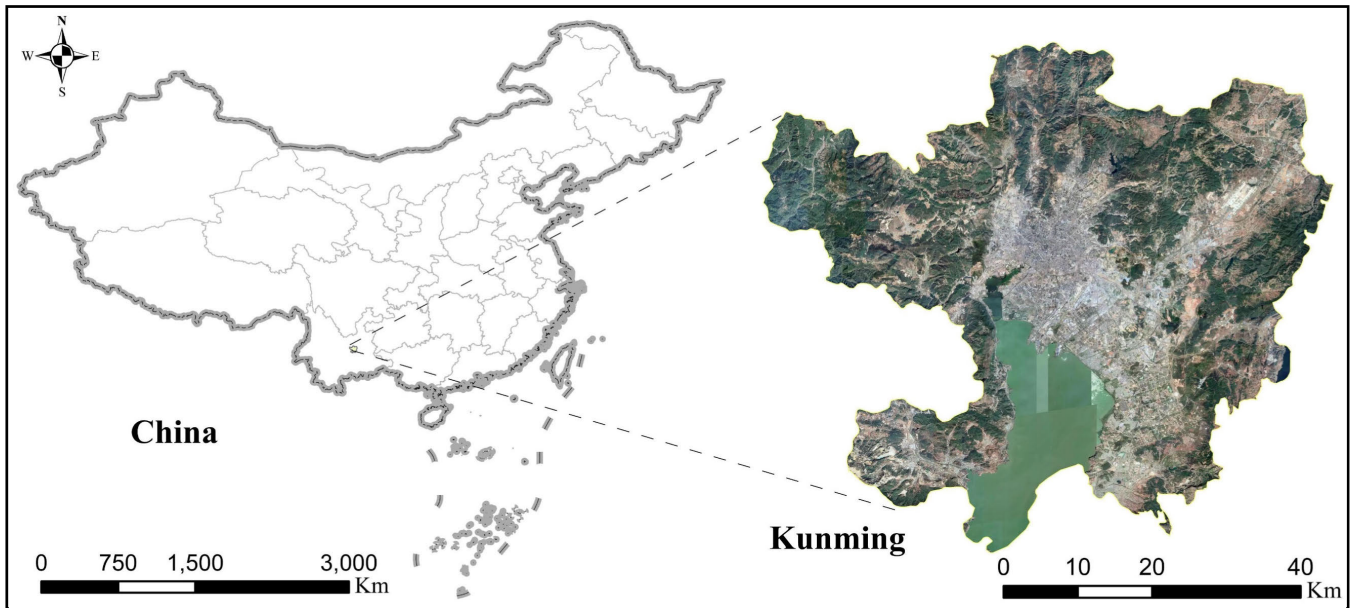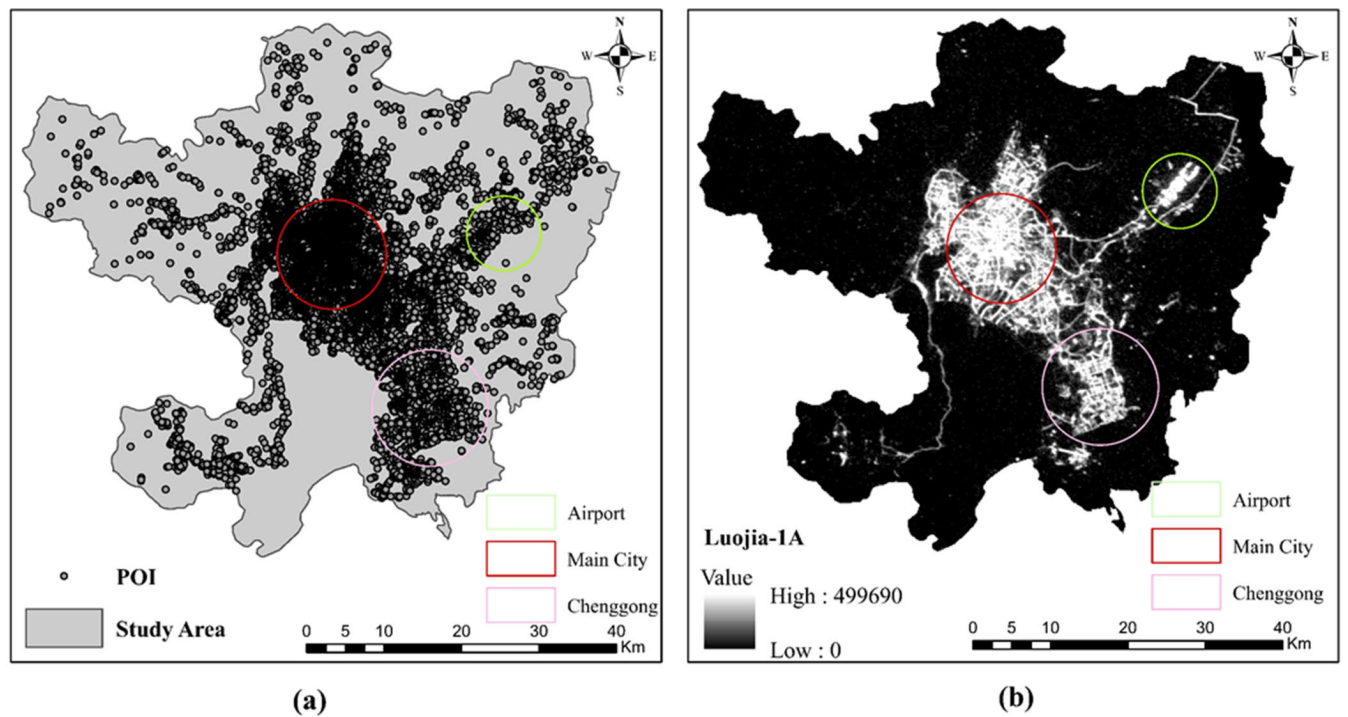
FIGURE 1. Research area.

FIGURE 2. POI data (a) and LuoJia-1A data (b) of 2019.

resolution of DMSP/OLS and NPP/VIIRS data and light overflow. In addition, the use of these data also provides light data for the extraction of individual cities and small and medium-sized urban built-up areas. The night light data of October 2018, December 2018, and March 2019 are obtained by this study from the Hubei Data and Application Network of the High-resolution Earth Observation System

(http://59.175.109.173:8888/index.html) (Luojia-1A data is available for download from October 2018, and before March 2019, data in the study area can only be obtained for the three periods of October 2018, December 2018, and March 2019), and the night light data of (FIGURE2, b) of FIGURE 2 (a) is obtained on the basis of averaging the data of the three periods.

2) POI DATA

POIs refer to all urban entities abstracted in geographic space. Each POI contains the attribute categories and longitude and latitude of an abstract urban entity, and the abstract urban entities basically cover all aspects of urban functions due to their very large number. The POI data used in this study are mainly from Amap (http://www.amap.com), which, as one of the three major map service providers in China, provides the most extensive and relatively accurate positioning services. In this study, with the help of the API interface provided by Amap, a total of 465,941 POI data points is obtained from the main urban area of Kunming in March 2019, as shown in FIGURE 2, b.

3) VERIFICATION DATA

1000 pixel points are randomly generated in the research area. Through data screening, it is determined that all the 1000 pixel points are located in Kunming. Besides, it is found that 281 of 1000 random points belong to urban built-up areas and 719 random points belong to non-built-up areas on the basis of field extraction of 1000 random points with the help of Google Earth.

IV. METHODS

A. OSTU THRESHOLD SEGMENTATION METHOD BASED ON GGM FUNCTION

In previous studies on the extraction of night-time light from urban built-up areas, different methods have often been used to determine the extraction threshold of night-time light. The reason for this is that the accurate selection of the night-time light threshold is considered to be most important. The night-time light data mainly contain the grey level information of the image, so the grey level segmentation algorithm of the image signal science can be used to segment the grey level characteristics of the night-time light. The OSTU algorithm is an efficient algorithm for image binarization proposed by Japanese scholar OSTU in 1979. To put it simply, the image grey level is set as 1 by default, the non-grey level is set as 0 by default, and the grey level feature is used for the binarization operation to extract the grey level of the image.

The basic idea of the OSTU algorithm is to divide the image into two parts according to the selected threshold: the target (grey level) and the background (non-grey level), calculate the maximum variance value corresponding to the pixel target and the background grey level, and take the threshold corresponding to the maximum variance value as the best threshold value.

The OSTU threshold segmentation method is a very good algorithm for image threshold segmentation for the following reasons: first, the OSTU threshold can be calculated by the MBV (maximum between-cluster variance) image; second, the OSTU algorithm has the advantages of a simple calculation, fast operation and effective results. Therefore, this aims hopes to use the OSGM algorithm based on the GGM (grey level and gradient mapping) function to detect the extraction
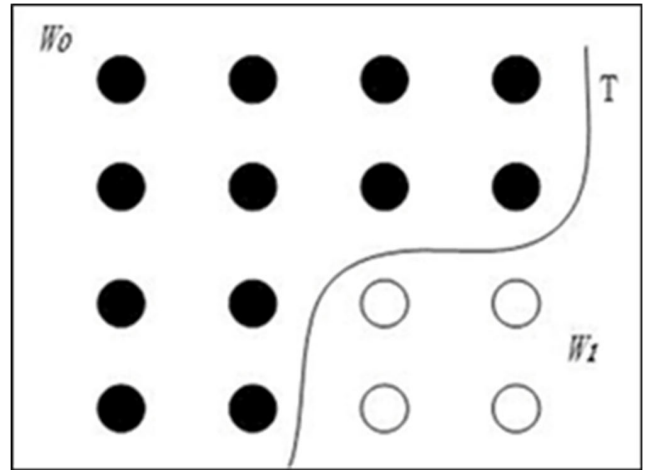

FIGURE 3. Segmentation model diagram based on OSTU algorithm.

threshold of night-time light [54], [55]. If α represents the greyscale value of the image and β represents the average gradient value of the image, then the mapping function $\beta = s(\alpha)$, where the mapping relation $s(\bullet)$ stands for the average gradient value level α of all pixels with greyscale.

As shown in FIGURE 3, the proportion of the background to the image is w_0 with an average grayscale of u_0; the proportion of the object to the image is w_1 with an average grayscale is u_1. If the total average grayscale of the image is u, and the variance of the segmentation scene and the reference scene is g, then T is the optimal segmentation threshold of the image background and object.

Suppose that the function $f(x, y)$ stands for the greyscale value of the pixel whose coordinate is (x, y) in the image and that its gradient value is defined by the two-dimensional vector as follows:

$$\nabla f = [\frac{\partial f}{\partial x} \frac{\partial f}{\partial y}] \tag{1}$$

The calculated value of the two-dimensional vector is:

$$\nabla f = \mathrm{mag}\,(\nabla f) = [G_x^2 + G_y^2]^{\frac{1}{2}} = [(\frac{\partial f}{\partial x})^2 + (\frac{\partial f}{\partial y})^2]^{\frac{1}{2}} \tag{2}$$

Suppose that the function $G(x, y)$ stands for the gradient function of the image; then, $G(x, y) = \nabla f$. Suppose that the number of pixels with greyscale i(i $\in [0; 1, \cdots L - 1]$, where L is the existing greyscale level) is n_i; then, its pixel set should be expressed as:

$$R_i = \{(x, y)|f(x, y) = i\} \tag{3}$$

Then, gray level and gradient mapping are defined as follows:

$$T(i) = \frac{\sum_{(x,y)\in R_i} G(x, y)}{n_i} i \in [0, 1, \cdots, L - 1] \tag{4}$$

where T stands for the average gradient and i for greyscale. Therefore, the mapping relationship between greyscale and gradient is established. That is, the OSTU algorithm based

on the GGM function obtains an appropriate segmentation threshold for the image.

B. DENSITY-GRAPH

POIs have different densities in different positions in the city. The density is higher in areas with higher urbanization and lower in areas with lower urbanization. In the actual spatial analysis, different density variables give different feedback to the spatial structure [56]. In a city, the density distribution of POIs will decrease from a built-up area to a non-built-up area, and the density of POIs will show an irreversible downward trend at the junction between the built-up area and the non-built-up area [50]. The breakpoint in this trend is the boundary between built-up and non-built-up areas. Since this trend is also an important connotation expressed by different spatial locations and densities, the density distribution of POIs in an urban space can directly reflect the spatial structure inside the city.

The basic idea of the density graph is to determine the critical value of the curve by constructing the relationship between the change in the POI curve value d and the theoretical radius $\Delta s_d \wedge (1/2)$ of the theoretical area Sd of the closed isoline. The steps of the density graph algorithm are as follows. First, it is necessary to determine the relationship between the density value d and the theoretical radius increment $\Delta s_d \wedge \left(1/2\right)$; the theoretical radius increment $\Delta s_d \wedge \left(1/2\right)$ needs to be derived, and then equation $lim \frac{d(\Delta S_d \wedge (1/2))}{dd}$ can be established. Second, it is necessary to judge the critical value of the density graph. In fact, the city is a very complex system. The vast majority of cities are composed of multiple city centres or more groups of non-uniform outward expansion, and the curve of point elements changes sharply in the urban space. Therefore, the performance of the density graph curve in the urban interior should fluctuate. However, from the perspective of the whole urban space on a macro scale, the fluctuation in the density-graph curve in urban space should be a critical point with overall significance. In other words, when $lim \frac{d(\Delta S_d \wedge (1/2))}{dd} > r$, that is, when the fluctuation of the density graph shows an irreversible growth trend, it can be considered that R is a critical point with overall significance, and this critical point is the critical value of the urban built-up area; then, the urban built-up area can be calculated.

As shown in FIGURE 4, the critical value of the POI number mutation is determined by constructing the density graph of the POI point density curve value d and the theoretical area S_d of the closed contour, the theoretical radius $\Delta s_d \wedge \left(1/2\right)$, if

$$lim \frac{d(\Delta S_d \wedge (1/2))}{dd} > r \qquad (5)$$

The density of POI will fluctuate (rise or fall) in the built-up area of the city. When the built-up area turns into the non-built-up area, the POI density generally decreases, and the decreasing trend is irreversible when the decreasing trend reaches a critical value. This is represented in the formula 5 as
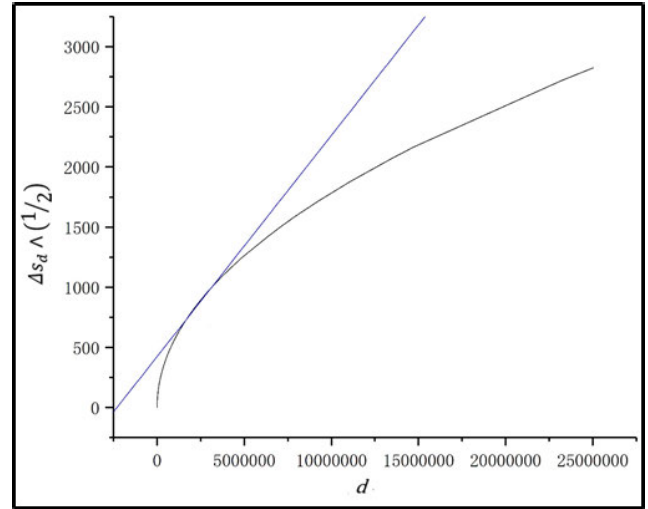

FIGURE 4. Density-graph model diagram.

when there is a limit value r after deriving the density value d of the closed POI density curve and the theoretical radius $\Delta s_d \wedge \left(1/2\right)$, and only when the POI density value is greater than the limit value r, it is a built-up area.

C. DATA INTEGRATION

There are shortcomings in only using night-time light data and only using POI data to extract urban built-up areas. For example, there are problems such as low spatial resolution and light overflow when only using night-time light data to extract urban built-up areas. Only using POI data would result in too high of a density difference between built-up and non-built-up areas. This is the reason why this study attempts to integrate the two kinds of data into new comprehensive data to extract urban built-up areas [51]. Integrated data for urban built-up areas are extracted by the density graph and OSTU threshold segmentation algorithms, and then the extraction accuracy of urban built-up areas with a single data source and integrated data can be judged separately.

In this study, the "geometric mean" is used to integrate night-time light data and POI data. The reason for this is that there is a considerable difference between the POI kernel density value and the DN value of night-time light, and there are noise points in the night-time light data. The use of the geometric mean in image integration can effectively eliminate the impact of image extremum and retain the original image information [57], so it is widely used in image integration [58]. The LJ & POI data after integration can eliminate the difference in the order of magnitude caused by the too-large density analysis value. Meanwhile, to some extent, these data can eliminate the background noise of night-time light images and reduce the influence of light overflow. The calculation formula is as follows:

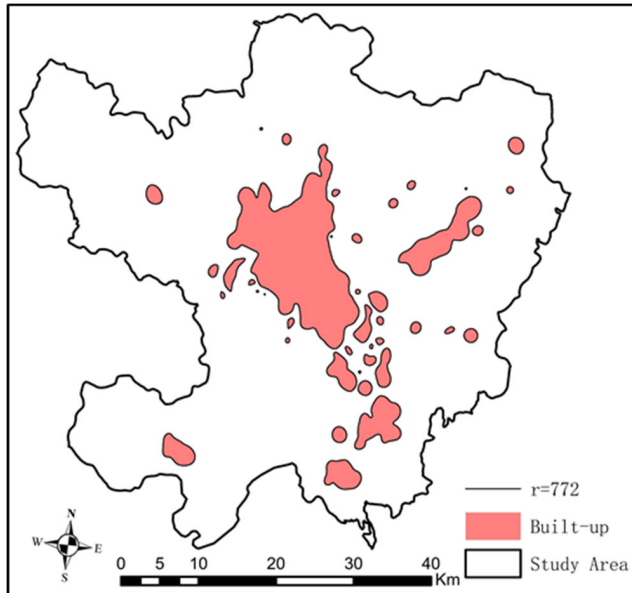$$POIDN_i = \sqrt{POI_i \times DN_i} \qquad (6)$$

where $POIDN_i$ is the composite index, POI_i is the POI kernel density value of point i, and DN_i is the night-time light brightness value of point i.

V. RESEACH RESULTS

A. URBAN BUILT-UP AREAS EXTRACTED BY DIFFERENT DATA

1) URBAN BUILT-UP AREAS EXTRACTED BY POI DATA

The spatial distribution of POIs in Kunming is obtained by the point density analysis of POIs. It can be concluded from FIGURE 5 that the POIs in the main urban area of Kunming present a spatial distribution pattern of decreasing circles. A high POI density is mainly found in regions with higher urbanization levels. With the decline in the urbanization level, the POI density also shows a decreasing trend. From the perspective of the overall spatial distribution of the POI point density in the study area, the distribution of POIs in urban space clearly follows is the rule that the POI density changes from dense to sparse from the urban center to the urban edge.

According to the POI density graph in FIGURE 5, the ratio relationship between the POI density and the theoretical radius is calculated by constructing a density graph. It is concluded that when the theoretical radius of POI density is 772, the POI density shows an irreversible downward trend. That is, when $r = 722$, the area enclosed by the POI density radius is the urban built-up area.

The area of the urban built-up area extracted by POIs is 381.68 square kilometers, and the circumference is 415.5 kilometers. The ratio of area to circumference is 0.92. The boundary of the extracted urban built-up area is of low complexity. Although the number of patches extracted from urban built-up areas is as many as 41, the internal details of urban built-up areas are not reflected in the patches of large

urban built-up areas, and the actual situation of urban built-up areas is not reflected in the patches of scattered urban built-up areas; however, the degree of plaque separation here is high. As seen from FIGURE 5 the distribution pattern of urban built-up areas in Kunming conforms to the pattern of urban built-up areas, urban fringe areas and non-built-up areas. Objectively speaking, urban built-up areas based on POI extraction generally generate smooth curves near the extracted boundary, with the shortcomings of simple edge details and serious information loss; therefore, the extraction results do not conform to the actual urban built-up areas.

In general, the urban built-up areas extracted by POI have significant improvements.
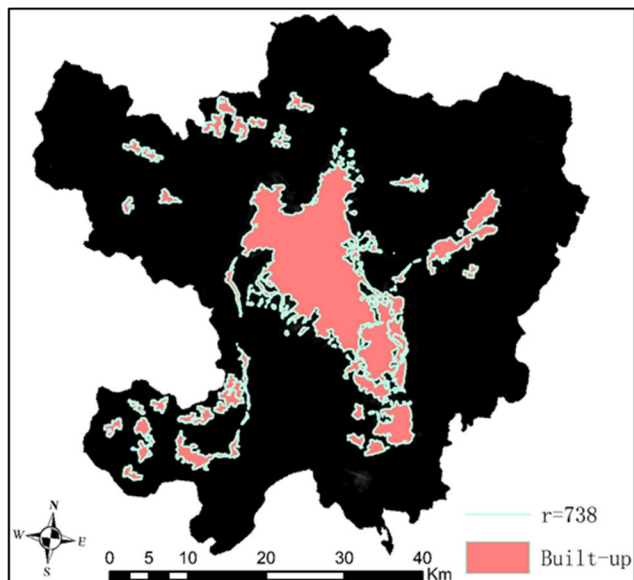
2) URBAN BUILT-UP AREAS EXTRACTED BY LUOJIA-1A DATA

It can be seen from the night-time light graph of LuoJia-1A in Kunming that the LuoJia-1A data can be used to clearly sketch the outline of urban built-up areas in Kunming, and the brightness of night-time light is obviously positively correlated with the urbanization level of the region. However, due to the high light value of the airport and the serious problem of light overflow in the whole city, it is difficult to determine the segmentation threshold of night-time light just through observation. The segmentation threshold can be calculated by the OSTU algorithm based on the GGM function, with the optimal segmentation threshold of night-time light of LuoJia-1A in Kunming city being $T(i) = 0.00063$, and the urban built-up area extracted by $T(i) = 0.00063$ is shown in FIGURE 6.

The area of the urban built-up area extracted by LuoJia-1A is 391.84 square kilometers, and the circumference is 706.98 kilometers. The ratio of area to circumference is 0.55, which shows that the complexity of the boundary of the extracted urban built-up area has been improved. Although the total number of plaques extracted in the urban built-up areas is as many as 96, most of the built-up area plaques are severely fragmented, and the extraction of urban built-up areas is severely disturbed, except for the plaques of the urban built-up area of the three major cities of Chenggong New Town, the airport, and the central city. It can be seen from FIGURE 6 that the edge details of urban built-up areas extracted by night-time light are too complex, and there is too much interference information inside. In addition, there is the problem of light overflow, which interferes with the extraction of urban built-up areas. Although the urban built-up area is roughly the same, the boundary details are more complex compared with the urban built-up area extracted by POI data.

3) URBAN BUILT-UP AREAS EXTRACTED BY SIMPLE INTEGRATION OF DATA

By simply integrating POI data with LJ-1A data, new integrated LJ_POI data can be obtained. Then, by performing density graph and OSTU analysis on the integrated data, the urban built-up area extracted in FIGURE 7,a can be obtained. If the theoretical radius of the urban built-up area

FIGURE 6. Urban built-up areas extracted by LuoJia-1A data.

is extracted by the density graph $r = 691$, the density curve shows an irreversible declining trend. The area of the urban built-up area extracted by LJ_POI data based on the density graph is 401.28 square kilometers, the circumference is 679.3 kilometers, and the perimeter area ratio is 0.59. The number of extracted urban built-up area patches is 60. The internal and marginal details of the extracted urban built-up area are improved, and the extraction of urban built-up area is also more accurate.

The segmentation threshold of LJ_POI data can be determined by using the algorithm, which is calculated by the OSTU algorithm based on the GGM function. When the segmentation threshold $T(i)$ is 633.21, the algorithm achieves the best effect (FIGURE 7, b). The urban built-up area extracted from the LJ & POI data based on the OSTU algorithm of the GGM function is 407.2 square kilometers, with a circumference of 643.72 kilometers and an area circumference ratio of 0.63. The extracted built-up area boundary becomes less complex. The number of extracted plaques in urban built-up areas is 53, and not only is the degree of plaque fragmentation increased compared with that of the single data source but the void in urban built-up areas is also reduced. All these results indicate that data integration has improved the extraction of urban built-up areas in edges and details.

Compared with the urban built-up areas extracted by POI and Luojia-1A, the urban built-up areas extracted after simple integration of data are all more accurate in terms of the area, perimeter, number of patches and edge details.

4) THE URBAN BUILT-UP AREA EXTRACTED AFTER THE INTEGRATION OF GEOMETRIC MEAN OF THE DATA

The new integrated LJ & POI data (FIGURE 8), are obtained by the integration calculation of the geometric mean value between the POI data and the LuoJia-1A data. It can be found

through observation that the LJ & POI data combine the advantages of two kinds of data: namely, it has the stability and effectiveness of POI data while further eliminating the influence of light noise. Compared with LuoJia-1A data, LJ & POI data significantly improve the problem of light spillover. In addition, the expression of internal details, including urban streets, is clearer and more complete. Compared with POI data, LJ & POI data have more real urban internal expressions and richer urban boundaries. In general, from the perspective of the data integration effect, the integrated LJ & POI data can more accurately express the urban built-up area.

Through the construction of the density graph analysis of LJ & POI data and the comparison of the relationship between the added value of LJ & POI density and the theoretical radius, it is concluded that when $r = 738$, the density extracted by the LJ & POI data presents an irreversible downward trend. The urban built-up area extracted based on $r = 738$ is shown in FIGURE 9,a.

The area of the urban built-up area extracted by the LJ & POI data based on the density graph is 413.46 square kilometers with a perimeter of 669.7 kilometers. The ratio of area to circumference is 0.62, which shows that the complexity of the boundary of the extracted urban built-up area is slightly high. Although the total number of urban built-up area plaques extracted is as many as 64, the urban built-up area plaques are well separated, and the internal details of the extracted urban built-up area are clear, especially in the urban boundary zone. Due to the improvement of the complexity of the urban boundary, the effect of extraction is closer to the real situation of the urban built-up areas, and the urban built-up area is better expressed.

The segmentation threshold of the LJ & POI data can be calculated by using the OSTU algorithm based on the GGM function. It can be seen from the algorithm calculation that when the segmentation threshold $T(i)$ is 672.38, the algorithm obtains the best result, so the area with pixel value greater than 672.38 is the urban built-up area (FIGURE 9,b).

The area of the extracted urban built-up area extracted by the OSTU algorithm based on the GGM function of LJ & POI is 405.05 square kilometers with a perimeter of 635.65 kilometers. The ratio of area to circumference is 0.62, which shows that the complexity of the boundary of the extracted urban built-up area is reduced. Although the total number of plaques extracted from the urban built-up area is as many as 52, the degree of plaque fragmentation in the urban built-up area is reduced, and the gaps in the urban built-up area are well compensated within the city. As seen from FIGURE 9,b, the urban built-up area extracted based on the LJ & POI data can better express the urban built-up area, and the complex interference information of the boundary of the urban built-up area extracted from the integrated data is less, which makes the extracted built-up area closer to the real built-up area and the internal details of the extracted built-up area closer to the real built-up area; the inner details of the city are also improved.
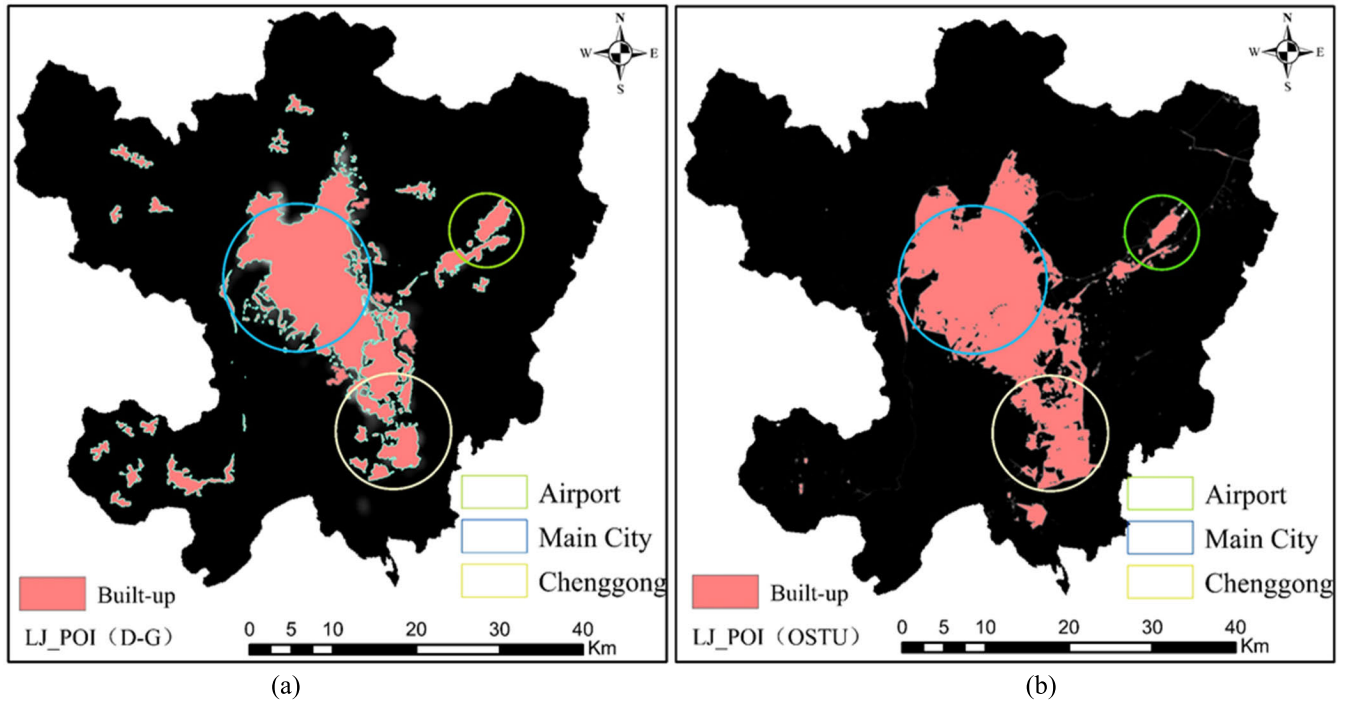
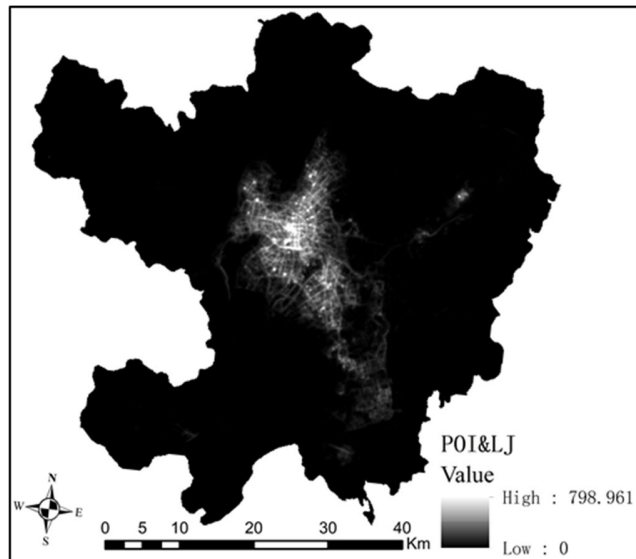**FIGURE 7.** Urban built-up areas extracted by LJ_POI.

FIGURE 8. Integrated LJ & POI data.

B. COMPARISON OF EXTRACTION RESULTS

After the extraction and comparison of the results of urban built-up areas extracted in the above chapters, it is found that there are subtle differences among the urban built-up areas extracted by different data, but their approximate ranges are the same as shown in FIGURE 10 The subtle difference in the overall performance among the data sources is that the effect of urban built-up areas extracted by the integrated data is better than that of urban built-up areas extracted by a single

data source. In addition, the result of data recognition based on geometric mean integration is better than the result of simple data integration recognition. The extracted detailed built-up area data are shown in Table 1.

According to FIGURE 10 and Table 1, the overall effect of urban built-up areas extracted after data integration is better than that before data integration. The extracted urban built-up area shows that the data effect of geometric mean integration is greater than that of simple data integration and greater than that of a single data source, while the same data extracted based on two different methods shows little difference in the urban built-up areas.

Comparing the urban built-up areas extracted by POI and LuoJia1-A data, it can be found that the urban built-up areas extracted by LuoJia-1A data are superior to the urban built-up areas extracted by POI data in terms of different indexes. However, the urban built-up areas extracted by these two kinds of data also have some shortcomings. First, the perimeter of the urban built-up areas extracted by POI data is relatively short, and the details of the boundaries of the urban built-up areas are relatively simple. The urban built-up area extracted by LuoJia-1A data is too complicated, with the number of plaques reaching 96, which seriously interferes with the extraction of real urban built-up areas.

There is a principle that the living and related auxiliary facilities in the area with high urbanization are relatively high, while in areas with lower urbanization, the number of related facilities is relatively low. Objectively, there will be a sharp drop in the number of POIs at the boundary of urban built-up areas extracted by POI data, but, this trend, which mainly
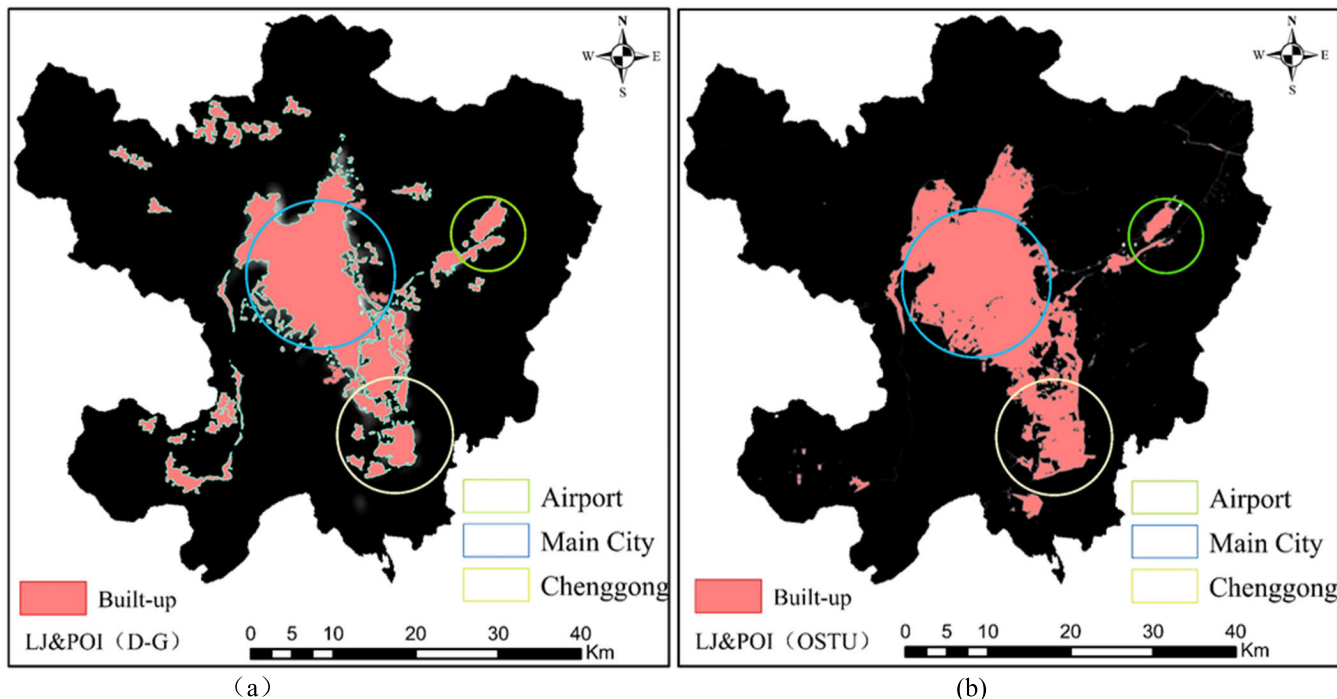
（a）

（b）

**FIGURE 9.** Built-up area extracted by LJ&POI data based on the density graph.

TABLE 1. Urban built-up areas extracted by different data.

	Area(km^2)	Perimeter(km)	Area/Perimeter	Number of Plaques in Built-up Area
POI	381.68	415.5	0.92	41
LuoJia-1A	391.84	706.98	0.55	96
LJ & POI (D-G) (Simple Integration)	401.28	679.3	0.59	60
LJ & POI (OSTU) (Simple Integration)	407.2	643.72	0.63	53
LJ&POI(D-G) (Integration of Geometric Mean)	413.46	669.7	0.62	64
LJ&POI(OSTU) (Integration of Geometric Mean)	405.05	653.65	0.62	52

depends on the decline of urbanization, is not as obvious in urban built-up areas because there are still many urban built-up areas in zones with low urbanization. Not only will urban built-up areas extracted by POIs have distorted details at the edges but the extracted urban built-up areas will also be small. The LuoJia1-A data are based on the principle that the higher the night-time light value is, the greater the probability that the relevant area belongs to the urban built-up area. Therefore, objectively speaking, areas with light value belong to urban built-up areas; however, for actual urban night-time light, in addition to the strong light from airports and ports, which will affect the final built-up area extraction results, there will also be light overflow and a light hole phenomenon in the city interior, which will further interfere with the extraction of urban built-up areas.

Comparing the urban built-up areas extracted by different data (FIGURE 10), it is found that although there are differences in the scope of urban built-up areas extracted

by different data, the main differences mainly exist in the following four major locations: the Changshui airport (FIGURE 10,1), Luosiwan(FIGURE 10,2), Chenggong New Town(FIGURE 10,3), and Xishan District(FIGURE 10,4). Because the Changshui airport is an aviation center and the development of other urban-related facilities is slow except for aviation-related facilities, although there are relatively large urban built-up area plaques in the results of LuoJia1-A extraction, the results are quite different from the results of POI extraction. Although Chenggong New Town, the seat of the Kunming municipal government and the university center, has been vigorously constructed in recent years, the development of relevant urban facilities cannot be compared with the speed of urban construction, which makes the urban built-up areas extracted by POI and LuoJia-1A data relatively smaller because of the impact of urbanization. The situation of Luosiwan is similar to that of Chenggong New Town. Due to its proximity to Dianchi Lake and the elegant nat-
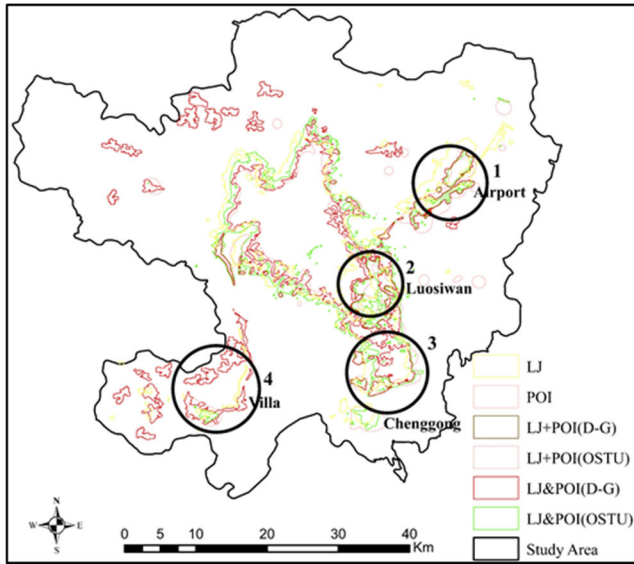
FIGURE 10. Comparison of urban built-up areas extracted by different data.

ural environment, most of the villas in Kunming are built in Xishan District; thus, although the urban built-up area and urban related facilities in Xishan district are gradually developing, the light intensity value at night is weak, which leads to great differences in the urban built-up area extracted by LuoJia-1A data.

C. VERIFICATION AND COMPARISON OF ACCURACY RESULTS

The verification of accuracy results is the most important step to test the reliability of experimental results. In this study, conintegration matrix and overall accuracy are used to verify the urban accuracy extracted by POI, LuoJia-1A, LJ_POI, LJ&POI data respectively. The accuracy verification of the extracted conintegration matrix is shown in Table 2.

As can be seen from Table 2, the highest accuracy in extracting urban built-up areas by single data is the POI and Luojia-1A data integrated by geometric mean, and the overall accuracy verified is 88.8% and 91.4% respectively, and the Kappa coefficient is 0.91 and 0.86 respectively. The second highest accuracy is obtained by simply integrating POI data and Luojia-1A data with the verified overall accuracy of 84.6% and 83.1% respectively, and the Kappa coefficient of 0.77 and 0.79 respectively. The data with the lowest verification accuracy are the POI data and the Luojia-1A data with the verification accuracy of only 73.9% and 74.3% respectively, and the Kappa coefficient of only 0. 47 and 0.54 respectively, so the fitting effect is too low.

It can be found through accuracy verification that the overall accuracy of single data extraction of urban built-up areas is general, but the Kappa coefficient is too low, which proves the limitation of single data extraction in urban built-up areas. After the integration of POI data and Luojia-1A data, the accuracy reaches over 85% and the Kappa coefficient reaches

over 0.75, which proves the superiority of data integration in urban built-up area extraction. Among which, the data integration method based on geometric mean proposed in this study has the best effect.

VI. DISCUSSION

In this study, POI data, LuoJia-1A data and integrated data are used to extract the urban built-up area of the main urban area of Kunming. This study posits that the urban built-up areas extracted by the POI data and LuoJia-1A data based on the density graph and GGM functions of the OSTU algorithm, respectively, all supplement the deficiencies of the previously extracted data and methods of urban built-up areas. First, the use of POI big data based on a density graph is reliable for extracting urban built-up areas, as this method objectively eliminates the subjective thresholds set arbitrarily in the previous data and the scale effect under the spatial scale. The case study of Kunming proves the value of POI big data in exploring urban space, especially in urban built-up areas. Second, the night-time light data of LuoJia-1A are used to extract urban built-up areas, which, on the one hand, makes up for the lack of research on night-time light data in small and medium-sized cities due to the spatial resolution and, on the other hand, provides a case study on the use of LuoJia-1A data. The conclusion of this study can be further extended to a large number of cities in China and provide effective practical experience for the study of urban built-up areas. Compared with the latest relevant research results, the overall extraction accuracy of the global artificial impairment area (GAIA) is greater than 90% on a global scale [59], while the accuracy of the urban built-up area extracted in this study is 91.4%, closing to the overall accuracy of the relevant researchers conducted by Gong and his team, which shows that the integrated data of this study has high accuracy in extracting urban built-up areas, therefore the extracted urban built-up areas can also be applied to related research and analysis of urban spatial structure [60]. However, since this study focuses on the extraction of urban built-up areas at the microscopic scale under a single city, the coarse resolution of night lights determines the limitation of the extraction accuracy of urban built-up areas at the microscopic scale [61], so the results of this study are more practical in the refined urban scale.

In addition, the integrated LJ & POI data are proposed in this study based on POI data and LuoJia-1A data, which provide a better solution. Finally, the new integrated data have also achieved good results in the practical application of extraction studies of urban built-up areas, which will play a useful role in future research on urban built-up areas. However, compared with traditional data, integrated data have still been the subject of little research, and further theoretical and practical research on data integration should be conducted. This is a process of continuous exploration.

There are still some deficiencies in this study that need to be further improved. First, in terms of the use of POI big data, in this study, the weighted measure of POI data in space is assumed to be consistent, but as a geographic entity point,

TABLE 2. Conintegration matrix and kappa coefficient.

Data		Built-up Area	Non-built-up Area	Overall accuracy	Kappa
POI	Built-up Area	142	221	73.90%	0.47
	Non-built-up Area	139	498		
Luojia-1A	Built-up Area	144	208	74.30%	0.54
	Non-built-up Area	137	511		
LJ_POI（D_G）	Built-up Area	162	140	84.60%	0.77
	Non-built-up Area	119	579		
LJ_POI（OSTU）	Built-up Area	171	153	83.10%	0.79
	Non-built-up Area	110	566		
LJ&POI（D_G）	Built-up Area	251	78	89.80%	0.86
	Non-built-up Area	30	641		
LJ&POI（OSTU）	Built-up Area	267	37	91.40%	0.91
	Non-built-up Area	14	682		

the entity category represented by each point of POI should be unequal. It is not discussed here whether there will be deviations from the existing results in the extraction of urban built-up areas if the spatial weights of POI data are considered separately. Second, the data integration method proposed in this study is not suitable for the analysis of long-term span evolution because the time series of POI data is very short, but both the POI data and LJ & POI data in this study include POI data. Therefore, in future research, multiple data integrations should be properly considered for the long-term monitoring of changes in urban built-up areas.

VII. CONCLUSION

Based on POI data and Luojia-1A data, this research proposes a new method that integrates the two data to extract urban built-up areas. The built-up areas are extracted by POI data, Luojia-1A data and the integration of the two kinds of data. Finally, 1000 random verification points are used to verify and analyze. Therefore, it can be concluded that data integration can not only provide a new method and approach for the extraction of urban built-up areas, but also play an active role in guiding the actual planning and construction of future cities.

AUTHOR CONTRIBUTIONS

In the process of this research, the main contribution of Z, J was the first draft and the final draft, Y, X-D was responsible for model processing, data collection and picture typesetting, L, H was responsible for picture typesetting and document typesetting.

CONFLICTS OF INTEREST

The authors declare no conflict of interest.

REFERENCES

[1] W. Yu, Y. Zhang, W. Zhou, W. Wang, and R. Tang, "Urban expansion in Shenzhen since 1970s: A retrospect of change from a village to a megacity from the space," *Phys. Chem. Earth, A/B/C*, vol. 110, pp. 21–30, Apr. 2019.

[2] Y. Sun and S. Zhao, "Spatiotemporal dynamics of urban expansion in 13 cities across the Jing-Jin-Ji urban agglomeration from 1978 to 2015," *Ecol. Indicators*, vol. 87, pp. 302–313, Apr. 2018.

[3] B. Chen, Y. Song, B. Huang, and B. Xu, "A novel method to extract urban human settlements by integrating remote sensing and mobile phone locations," *Sci. Remote Sens.*, vol. 1, Jun. 2020, Art. no. 100003.

[4] W. Li, H. Liu, Y. Wang, Z. Li, Y. Jia, and G. Gui, "Deep learning-based classification methods for remote sensing images in urban built-up areas," *IEEE Access*, vol. 7, pp. 36274–36284, 2019.

[5] F. Zhen, S.-Q. Zhang, X. Qin, and G.-L. Xi, "From informational empowerment to comprehensive empowerment: Exploring the ideas of smart territorial spatial planning," *J. Natural Resour.*, vol. 34, no. 10, pp. 2060–2072, 2019.

[6] X. Qin, F. Zhen, Y. Li, and H. Chen, "Discussion on the application framework of big data in territorial spatial planning," *J. Natural Resour.*, vol. 34, no. 10, pp. 2134–2149, 2019.

[7] L. Liu and Y. Leung, "A study of urban expansion of prefectural-level cities in South China using night-time light images," *Int. J. Remote Sens.*, vol. 36, no. 22, pp. 5557–5575, Nov. 2015.

[8] X. Ma, X. Tong, S. Liu, X. Luo, H. Xie, and C. Li, "Optimized sample selection in SVM classification by combining with DMSP-OLS, Landsat NDVI and GlobeLand30 products for extracting urban built-up areas," *Remote Sens.*, vol. 9, no. 3, p. 236, Mar. 2017.

[9] B. Yu, M. Tang, Q. Wu, C. Yang, S. Deng, K. Shi, C. Peng, J. Wu, and Z. Chen, "Urban built-up area extraction from log-transformed NPP-VIIRS nighttime light composite data," *IEEE Geosci. Remote Sens. Lett.*, vol. 15, no. 8, pp. 1279–1283, Aug. 2018.

[10] M. Luqman, P. J. Rayner, and K. R. Gurney, "Combining measurements of built-up area, nighttime light, and travel time distance for detecting changes in urban boundaries: Introducing the BUNTUS algorithm," *Remote Sens.*, vol. 11, no. 24, p. 2969, Dec. 2019.

[11] T. Hu and X. Huang, "A novel locally adaptive method for modeling the spatiotemporal dynamics of global electric power consumption based on DMSP-OLS nighttime stable light data," *Appl. Energy*, vol. 240, pp. 778–792, Apr. 2019.

[12] L. Wang, H. Fan, and Y. Wang, "Fine-resolution population mapping from international space station nighttime photography and multisource social sensing data based on similarity matching," *Remote Sens.*, vol. 11, no. 16, p. 1900, Aug. 2019.

[13] Z. Chen, B. Yu, Y. Zhou, H. Liu, C. Yang, K. Shi, and J. Wu, "Mapping global urban areas from 2000 to 2012 using time-series nighttime light data and MODIS products," *IEEE J. Sel. Topics Appl. Earth Observ. Remote Sens.*, vol. 12, no. 4, pp. 1143–1153, Apr. 2019.

[14] W. Yue, S. Qiu, H. Xu, L. Xu, and L. Zhang, "Polycentric urban development and urban thermal environment: A case of Hangzhou, China," *Landscape Urban Planning*, vol. 189, pp. 58–70, Sep. 2019.

[15] H.-M. Li, X.-G. Li, X.-Y. Yang, and H. Zhang, "Analyzing the relationship between developed land area and nighttime light emissions of 36 Chinese cities," *Remote Sens.*, vol. 11, no. 1, p. 10, Dec. 2018.

[16] C. Yang, B. Yu, Z. Chen, W. Song, Y. Zhou, X. Li, and J. Wu, "A spatial-socioeconomic urban development status curve from NPP-VIIRS night-time light data," *Remote Sens.*, vol. 11, no. 20, p. 2398, Oct. 2019.

[17] T. Ma, C. Zhou, T. Pei, S. Haynie, and J. Fan, "Quantitative estimation of urbanization dynamics using time series of DMSP/OLS nighttime light data: A comparative case study from China's cities," *Remote Sens. Environ.*, vol. 124, pp. 99–107, Sep. 2012.

[18] B. Yu, S. Shu, H. Liu, W. Song, J. Wu, L. Wang, and Z. Chen, "Object-based spatial cluster analysis of urban landscape pattern using nighttime light satellite images: A case study of China," *Int. J. Geograph. Inf. Sci.*, vol. 28, no. 11, pp. 2328–2355, Nov. 2014.

[19] X. Liu, A. de Sherbinin, and Y. Zhan, "Mapping urban extent at large spatial scales using machine learning methods with VIIRS nighttime light and MODIS daytime NDVI data," *Remote Sens.*, vol. 11, no. 10, p. 1247, May 2019.

[20] X. Li, H. Xu, X. Chen, and C. Li, "Potential of NPP-VIIRS nighttime light imagery for modeling the regional economy of China," *Remote Sens.*, vol. 5, no. 6, pp. 3057–3081, Jun. 2013.

[21] J. Ou, X. Liu, X. Li, M. Li, and W. Li, "Evaluation of NPP-VIIRS nighttime light data for mapping global fossil fuel combustion CO_2 emissions: A comparison with DMSP-OLS nighttime light data," *PLoS ONE*, vol. 10, no. 9, 2015, Art. no. e0138310.

[22] K. Shi, B. Yu, Y. Huang, Y. Hu, B. Yin, Z. Chen, L. Chen, and J. Wu, "Evaluating the ability of NPP-VIIRS nighttime light data to estimate the gross domestic product and the electric power consumption of China at multiple scales: A comparison with DMSP-OLS data," *Remote Sens.*, vol. 6, no. 2, pp. 1705–1724, Feb. 2014.

[23] L. Wang, R. Chen, D. Li, G. Zhang, X. Shen, B. Yu, C. Wu, S. Xie, P. Zhang, M. Li, and Y. Pan, "Initial assessment of the LEO based navigation signal augmentation system from Luojia-1A satellite," *Sensors*, vol. 18, no. 11, p. 3919, Nov. 2018.

[24] Y. Liu, X. Liu, S. Gao, L. Gong, C. Kang, Y. Zhi, G. Chi, and L. Shi, "Social sensing: A new approach to understanding our socioeconomic environments," *Ann. Assoc. Amer. Geographers*, vol. 105, no. 3, pp. 512–530, May 2015.

[25] Q. Zhang, C. Schaaf, and K. C. Seto, "The vegetation adjusted NTL urban index: A new approach to reduce saturation and increase variation in nighttime luminosity," *Remote Sens. Environ.*, vol. 129, pp. 32–41, Feb. 2013.

[26] J. Peng, S. Zhao, Y. Liu, and L. Tian, "Identifying the urban-rural fringe using wavelet transform and kernel density estimation: A case study in Beijing City, China," *Environ. Model. Softw.*, vol. 83, pp. 286–302, Sep. 2016.

[27] A. Z. Kotarba and S. Aleksandrowicz, "Impervious surface detection with nighttime photography from the international space station," *Remote Sens. Environ.*, vol. 176, pp. 295–307, Apr. 2016.

[28] E. Al Nuaimi, H. Al Neyadi, N. Mohamed, and J. Al-Jaroodi, "Applications of big data to smart cities," *J. Internet Services Appl.*, vol. 6, no. 1, pp. 1–15, 2015.

[29] X. He, Z. Yang, K. Zhang, P. Yang, and S. Zhang, "The spatial distribution patterns of the catering trade in nanchang based on Internet public reviews," *Int. J. Technol.*, vol. 9, no. 7, pp. 1319–1328, 2018.

[30] F. Al-Turjman, L. Mostarda, E. Ever, A. Darwish, and N. S. Khalil, "Network experience scheduling and routing approach for big data transmission in the Internet of Things," *IEEE Access*, vol. 7, pp. 14501–14512, 2019.

[31] R. Chen, Q. Wang, and W. Xu, "Mining user requirements to facilitate mobile app quality upgrades with big data," *Electron. Commerce Res. Appl.*, vol. 38, Nov. 2019, Art. no. 100889.

[32] C. He, L. Ma, L. Zhou, H. Kan, Y. Zhang, W. Ma, and B. Chen, "Exploring the mechanisms of heat wave vulnerability at the urban scale based on the application of big data and artificial societies," *Environ. Int.*, vol. 127, pp. 573–583, Jun. 2019.

[33] X. Zhang, S. Du, and Q. Wang, "Hierarchical semantic cognition for urban functional zones with VHR satellite images and POI data," *ISPRS J. Photogramm. Remote Sens.*, vol. 132, pp. 170–184, Oct. 2017.

[34] G. R. Calegari, I. Celino, and D. Peroni, "City data dating: Emerging affinities between diverse urban datasets," *Inf. Syst.*, vol. 57, pp. 223–240, Apr. 2016.

[35] X. Kong, M. Li, T. Tang, K. Tian, L. Moreira-Matias, and F. Xia, "Shared subway shuttle bus route planning based on transport data analytics," *IEEE Trans. Autom. Sci. Eng.*, vol. 15, no. 4, pp. 1507–1520, Oct. 2018.

[36] Y. Xiao, D. Wang, and J. Fang, "Exploring the disparities in park access through mobile phone data: Evidence from Shanghai, China," *Landscape Urban Planning*, vol. 181, pp. 80–91, Jan. 2019.

[37] X. Song, R. Guo, T. Xia, Z. Guo, Y. Long, H. Zhang, X. Song, and S. Ryosuke, "Mining urban sustainable performance: Millions of GPS data reveal high-emission travel attraction in Tokyo," *J. Cleaner Prod.*, vol. 242, Jan. 2020, Art. no. 118396.

[38] F. Zhen, Y. Cao, X. Qin, and B. Wang, "Delineation of an urban agglomeration boundary based on Sina Weibo Microblog 'check-in' data: A case study of the Yangtze River Delta," *Cities*, vol. 60, pp. 180–191, Feb. 2017.

[39] J. Liu, T. Li, P. Xie, S. Du, F. Teng, and X. Yang, "Urban big data fusion based on deep learning: An overview," *Inf. Fusion*, vol. 53, pp. 123–133, Jan. 2020.

[40] T. Shi, "Spatial data mining and big data analysis of tourist travel behavior," *Ingénierie des systèmes d Inf.*, vol. 24, no. 2, pp. 167–172, Jul. 2019.

[41] M. M. Rathore, A. Ahmad, A. Paul, and S. Rho, "Urban planning and building smart cities based on the Internet of Things using big data analytics," *Comput. Netw.*, vol. 101, pp. 63–80, Jun. 2016.

[42] Y. Li, G. Liu, Z.-L. Zhang, J. Luo, and F. Zhang, "CityLines: Designing hybrid hub-and-spoke transit system with urban big data," *IEEE Trans. Big Data*, vol. 5, no. 4, pp. 576–587, Dec. 2019.

[43] Y. Zhang, Q. Li, W. Tu, K. Mai, Y. Yao, and Y. Chen, "Functional urban land use recognition integrating multi-source geospatial data and cross-correlations," *Comput., Environ. Urban Syst.*, vol. 78, Nov. 2019, Art. no. 101374.

[44] C. Zeng, Y. Song, D. Cai, P. Hu, H. Cui, J. Yang, and H. Zhang, "Exploration on the spatial spillover effect of infrastructure network on urbanization: A case study in wuhan urban agglomeration," *Sustain. Cities Soc.*, vol. 47, May 2019, Art. no. 101476.

[45] Z. Yang and X. He, "Analysis of the evolution of urban center space based on POI: A case study of main area in kunming," *Urban Develop. Stud.*, vol. 26, no. 2, pp. 31–35, 2019.

[46] Z. Yang, H. Xiong, Z. Kun, and Z. Jun, "Analysis of the correlation between takeaway and urban space from the perspective of POI: A case study of main area in kunming," *Urban Develop. Stud.*, vol. 27, no. 2, pp. 13–17, 2020.

[47] W. Zhai, X. Bai, Y. Shi, Y. Han, Z.-R. Peng, and C. Gu, "Beyond word2vec: An approach for urban functional region extraction and identification by combining place2vec and POIs," *Comput., Environ. Urban Syst.*, vol. 74, pp. 1–12, Mar. 2019.

[48] X. Zhang, S. Du, and Z. Zheng, "Heuristic sample learning for complex urban scenes: Application to urban functional-zone mapping with VHR images and POI data," *ISPRS J. Photogramm. Remote Sens.*, vol. 161, pp. 1–12, Mar. 2020.

[49] Y. Liu, Y. Zhang, S. T. Jin, and Y. Liu, "Spatial pattern of leisure activities among residents in Beijing, China: Exploring the impacts of urban environment," *Sustain. Cities Soc.*, vol. 52, Jan. 2020, Art. no. 101806.

[50] Z. Xu and X. Gao, "A novel method for extracting the boundary of urban built-up areas with POI data," *Acta Geographica Sinica*, vol. 71, no. 6, pp. 928–939, 2016.

[51] G. Lou, Q. Chen, K. He, Y. Zhou, and Z. Shi, "Using nighttime light data and POI big data to detect the urban centers of Hangzhou," *Remote Sens.*, vol. 11, no. 15, p. 1821, Aug. 2019.

[52] J. Liu, Y. Deng, Y. Wang, H. Huang, Q. Du, and F. Ren, "Urban nighttime leisure space mapping with nighttime light images and POI data," *Remote Sens.*, vol. 12, no. 3, p. 541, Feb. 2020.

[53] Z. Yang, X. He, K. Zhang, and J. L. Zhang, "Sustainable urban space expansion in central Yunnan (China): Regional urban integration," *Int. J. Sustain. Develop. Planning*, vol. 15, no. 1, pp. 95–106, Jan. 2020.

[54] X. Xie, H. Xiong, J. Wang, N. Jiang, and F. Hu, "An improved floc image segmentation algorithm based on Otsu and particle swarm optimisation," *Int. J. Comput. Sci. Eng.*, vol. 15, no. 1, pp. 49–56, 2017.

[55] L. Qi, J. Wang, C. D. Li, and W. Liu, "Research on the image segmentation of icing line based on NSCT and 2-D OSTU," *J. Comput. Appl. Technol.*, vol. 57, no. 2, pp. 112–120, 2018.

[56] H. Yang, Y. Zhang, L. Zhong, X. Zhang, and Z. Ling, "Exploring spatial variation of bike sharing trip production and attraction: A study based on Chicago's Divvy system," *Appl. Geogr.*, vol. 115, Feb. 2020, Art. no. 102130.

[57] M. Shen, R. Wang, and W. Cao, "Joint sparse representation model for multi-channel image based on reduced geometric algebra," *IEEE Access*, vol. 6, pp. 24213–24223, 2018.

[58] H. Cao, P. Tao, H. Li, and J. Shi, "Bundle adjustment of satellite images based on an equivalent geometric sensor model with digital elevation model," *ISPRS J. Photogramm. Remote Sens.*, vol. 156, pp. 169–183, Oct. 2019.

[59] P. Gong, X. Li, J. Wang, Y. Bai, B. Chen, T. Hu, X. Liu, B. Xu, J. Yang, W. Zhang, and Y. Zhou, "Annual maps of global artificial impervious area (GAIA) between 1985 and 2018," *Remote Sens. Environ.*, vol. 236, Jan. 2020, Art. no. 111510.

[60] X. Liu, G. Hu, Y. Chen, X. Li, X. Xu, S. Li, F. Pei, and S. Wang, "High-resolution multi-temporal mapping of global urban land using Landsat images based on the Google Earth engine platform," *Remote Sens. Environ.*, vol. 209, pp. 227–239, May 2018.

[61] Z. Ouyang, P. Fan, and J. Chen, "Urban built-up areas in transitional economies of Southeast Asia: Spatial extent and dynamics," *Remote Sens.*, vol. 8, no. 10, pp. 1–19, 2016.

YUAN XIAO-DIE received the Bachelor of Science degree from the Department of Resource Management and Urban and Rural Planning, School of Tourism and Geographical Sciences, Yunnan Normal University, in 2018. She is currently pursuing the master's degree in urban and rural planning with the School of Architecture and Planning, Yunnan University. Her research interest includes urban geography.

ZHANG JUN received the B.E. degree from Tsinghua University, Beijing, China, in 1990, and the M.S. degree from Tongji University, Shanghai, China, in 1993. He is currently the Dean of the School of Architecture and Planning and a Professor-Level Senior Engineer with Yunnan University. From 2015 to 2020, he has committed to remote sensing and geographic information systems. His current research interest includes application of arterial intelligence in geographic information systems and remote sensing. He was the owner of Luban Award in China.

LIN HAN received the bachelor's degree from South China Agricultural University, Guangzhou, China, in 2018. She is currently pursuing the M.E. degree with Yunnan University, Yunnan, China. From 2014 to 2020, she has committed to landscape design. Her current research interest includes traditional settlement research, such as landscape genome maps of traditional settlements.

• • •